Electronic Supplementary Material

Superhydrophobic, photo-sterilize, and reusable mask based on graphene nanosheet-embedded carbon (GNEC) film

Zezhou Lin[1], Zheng Wang[2], Xi Zhang[1] (✉), and Dongfeng Diao[1]

[1] *Institute of Nanosurface Science and Engineering, Guangdong Provincial Key Laboratory of Micro/Nano Optomechatronics Engineering, Shenzhen University, Shenzhen 518060, China*
[2] *Shenzhen Anhio Medical Technology Co., Ltd, Shenzhen 518110, China*

Supporting information to https://doi.org/10.1007/s12274-020-3158-1

Experimental section

Deposition of GNEC film: The GNEC films were deposited on the Si substrate by electron cyclotron resonance (ECR) sputtering system with low energy electron irradiation. The GNEC films were deposited on the Si substrate by using the electron cyclotron resonance (ECR) sputtering system. The Si substrate was cleaned in acetone and ethanol bath successively by ultrasonic waves. Before film deposition, the vacuum chamber was pumped down to 8×10^{-5} Pa and the argon was inflated to keep the working pressure with 1×10^{-1} Pa. A bias voltage of −500 V was applied to the carbon target for attracting the sputtering ions. The substrate was applied with a positive bias to form the electron irradiation. To our best research, the high edge density of graphene nanosheet was fabricated by setting the substrate bias 40 V.

Fabrication of GNEC mask: The GNEC mask was fabricated by the ultrasonic extrusion method. Electric carving device (JINTIAN MCD-50) with 11000/min high-frequency varication was used for breaking the GNEC film from the Si substrate. The ultrasonic-extrusion system (RAETTS) was used to embed GNEC nanostructure in smooth fibers. The extrusion time is 10 seconds with the ultrasonic frequency of 40 kHz and the working power of 600W. (See **Fig. S4** for detail information)

Characterization of the GNEC mask: SEM: the microstructures of the fibers were observed by scanning electron microscopy (SEM, FEI, Scios). ***TEM:*** the nanostructures of the carbon films were observed by transmission electron microscopy (TEM, FEI, Titan Cubed Themis G2 300). ***Water contact angle:*** the static contact angle (CA) of the sample surface was measured by the drop method using deionized water with a volume of 5 μL. In this work, all contact angle measurements were carried out in the same environment. The test instrument was a DSA 100S drop shape analyzer manufactured by KRUSS. Three different positions were measured on each sample surface, and the average value was reported as the final data. ***Raman:*** the Raman spectra were obtained with a Horiba HR800 Evolution system under the excitation laser wavelength of 532 nm. ***Optical absorption:*** the optical absorption spectrum was measured by a Solar cell quantum efficiency testing system (ZOLIX, SCS100). ***Solar illumination:*** the light source is acquired with the USHIO EKE 21V (150W) illuminating lamp, the light intensity can be adjusted by setting the input voltage (0 to 21V). ***Temperature mapping:*** the surface temperatures of the samples were measured by a FOTRIC 368T infrared camera. The filtration efficiency was measure by filter material performance tester (PALAS, PMFT-1000).

1 Electron cyclotron resonance (ECR) sputtering system

Figure S1 Electron cyclotron resonance (ECR) sputtering system.

Address correspondence to zh0005xi@szu.edu.cn

The GNEC films were fabricated by using an electron cyclotron resonance (ECR) plasma sputtering system. With the assistant of the low-energy electrons, graphene nanosheets embedded in amorphous carbon grow perpendicularly to the substrate. The atomic model of three-layer graphene sheets indicates the GNs embedded in amorphous carbon. A 500W-power microwave was delivered into the vacuum chamber to generate the plasma at the argon pressure of 4×10^{-2} Pa. The mirror confinement magnetic field was applied to enhance the plasma density. A negatively biased glassy carbon target was sputtered by Ar^{+} ions to generate carbon species towards the substrate. The thickness was controlled by deposition time. The deposition time of 30 min was adopted in this work and the thickness is ~70 nm. A positive deposited voltage (V_{dep}) was applied to the substrate for attracting electrons. With the assistant of the low-energy electrons, graphene nanosheets embedded in amorphous carbon grow perpendicularly to the substrate. The electron energy was modulated by V_{dep} which affects the size and number of GNs. We prepared films under V_{dep}=20 V, 40 V, 60 V and 80 V.

2 FIB processing to observe the cross-section of GNEC film

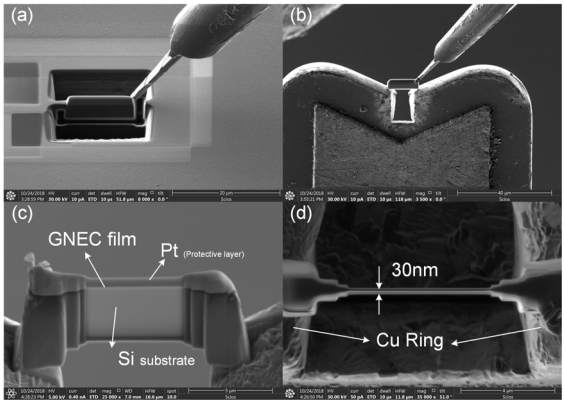

Figure S2 SEM images of (a) the origin cross-section sample, (b) the transferring cross-section sample. (c) the cross-section sample fabricated by using FIB, and sample located on a copper ring in preparation for TEM observation. (d) Top view of the cross-section, the thickness was thinned to 30 nm by ion irradiation.

The cross-section sample of 40 V GNEC film on the substrate was prepared by focused ion beam (FIB) etching. The protective layer is a layer of platinum having a thickness of 2 μm deposited on the surface of the sample by an auxiliary gas injection system associated with a FIB-SEM analysis system prior to FIB etching process. The lateral thickness of the cross-section sample was etched under 100 nm. As shown in the SEM image in **Fig. S2**, we prepare a cross-section sample with a thickness of about 30 nm, which is more conducive to our observation of the vertical growth structure of GNs under TEM. From the transmission electron microscopy (TEM) image of the cross-section sample, GNs grew vertically on the silicon substrate with a vertical thickness of ~70 nm.

3 TEM images to determine the graphene nanosheets (GNs) boundary

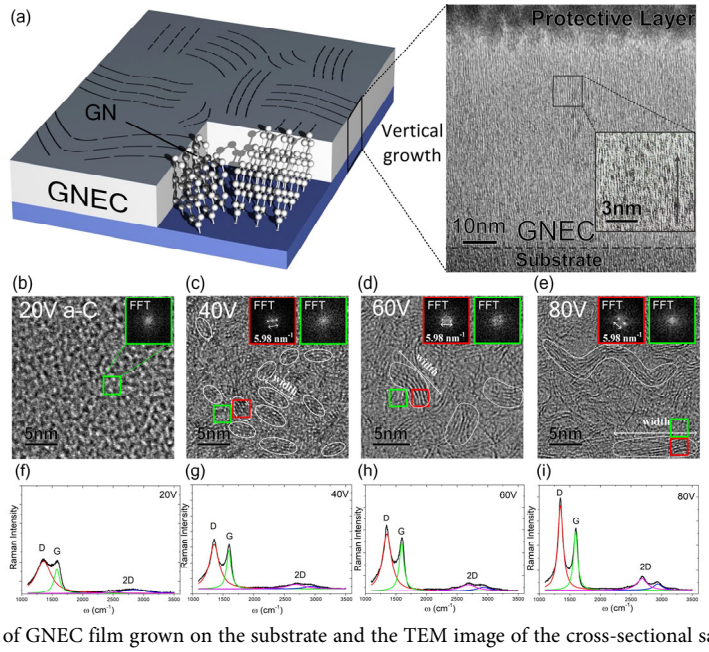

Figure S3 (a) Schematic diagram of GNEC film grown on the substrate and the TEM image of the cross-sectional sample prepared by FIB. Inset in the schematic diagram shows standing structured graphene nanosheets (GN) grown vertically on the Si substrate. High-resolution TEM plan-view images of GNEC films deposited at V_{dep} of (b) 20 V, (c) 40 V, (d) 60 V, and (e) 80 V. As the V_{dep} increases, GNs grow in width (as marked by white lines) among amorphous carbon film. Insets are the FFT images of the selected region (green and red squares). Raman Spectra of GNEC Films with V_{dep} of (f) 20 V, (g) 40 V, (h) 60 V, and (i) 80 V.

Fig. S3b-e shows the plan-view TEM images of films deposited at V_{dep} = 20V, 40V, 60V and 80 V. The energy of electrons was modulated by V_{dep} and calculated by e(V_{dep}-V_{plasma}), where V_{plasma} is the plasma potential measured as 10V. Red and green squares mark the regions inside and outside GN, as well as their fast Fourier transformation (FFT) images. FFT images show that inside the GN, two Laue spots appear corresponding to $(0001)^*$ facet of multilayer graphene. The reciprocal lattice distance $d^*_{(0001)}$ = 5.98/2 nm^{-1}=2.99 nm^{-1}, and the interplanar distance d = 1/2.99 nm = 0.334 nm, in accord with the (0001) facet distance of multilayer graphene. As the V_{dep} increases, irradiation electrons get higher energies to induce the growth of GNs. At V_{dep} = 20 V, the film is amorphous structure (a-C film) and contains a few GNs. At V_{dep} = 40 V, small-width GNs (≈ 3 nm) distribute randomly and densely among the film. At V_{dep} = 60 and 80 V, GN width grows to 7 and 15 nm on average. The crystallization of GNs enhanced by V_{dep} is verified by Raman spectra (**Fig. S3f-i**). At V_{dep} = 20V, the a-C film shows vague D and G peaks and no 2D band is observed. Above V_{dep} = 20V, the clear-shaped D band representing the long range ordered structure with sp^2 hybridization in amorphous structure. The intensity ratio of D peak over G peak (I_D/I_G) increases from 1.02 to 2.36 as the V_{dep} increases from 20 V to 80 V, indicating the increase of crystallization. Different from perfect graphene, in amorphous carbon film, D peak strength is proportional to the probability of finding a six-member ring, indicating ordering. In order to obtain the maximum edge density, the deposition voltage of 40 V for our considerations.

4 The schematic of ultrasonic system generator

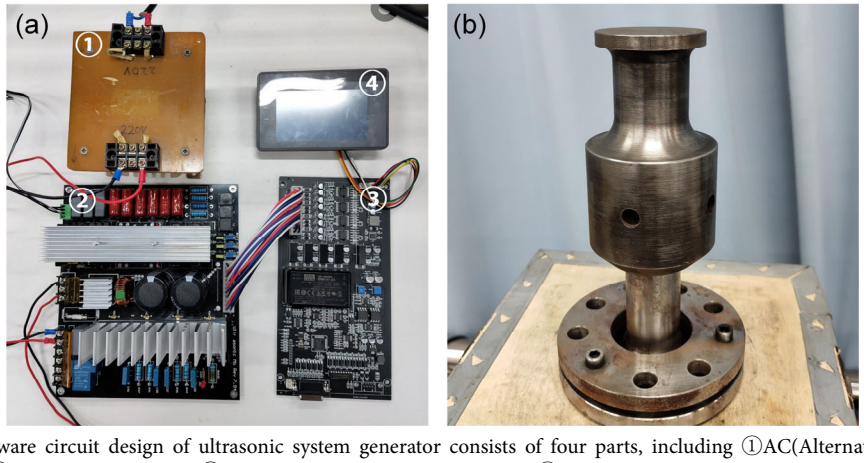

Figure S4 (a) The hardware circuit design of ultrasonic system generator consists of four parts, including ①AC(Alternating Current)--DC(Direct Current) transformer; ②The power amplifier; ③Control system for power amplifier; ④Touching screen. (b) Ultrasonic transducer.

The ultrasonic wave is used to convert high-frequency electrical energy into mechanical vibration through a transducer. As shown in Fig. S4, the current transformer is used for changing the AC to DC. The power amplifier converts direct current to high frequency high voltage. The output voltage can be controlled by a control system. People can input the expected output voltage signal by touching the screen. Finally, using an ultrasonic transducer, high frequency and high voltage can output ultrasonic wave stably.

Advantage of Generator: All-digital integrated circuit, using high-performance anti-interference processor, while reducing the number of components, simplifying the hardware structure, and increasing the voltage regulator function to improve the reliability and stability of the system. The application of IGBT power module and the structure of other excited oscillation circuits make the output power more than 1.5 times of the traditional self-excited circuit. Using amplitude stepless adjustment, The setting range of amplitude is 10% ~ 100%.

5 Ultrasonic extrusion process of GNEC mask

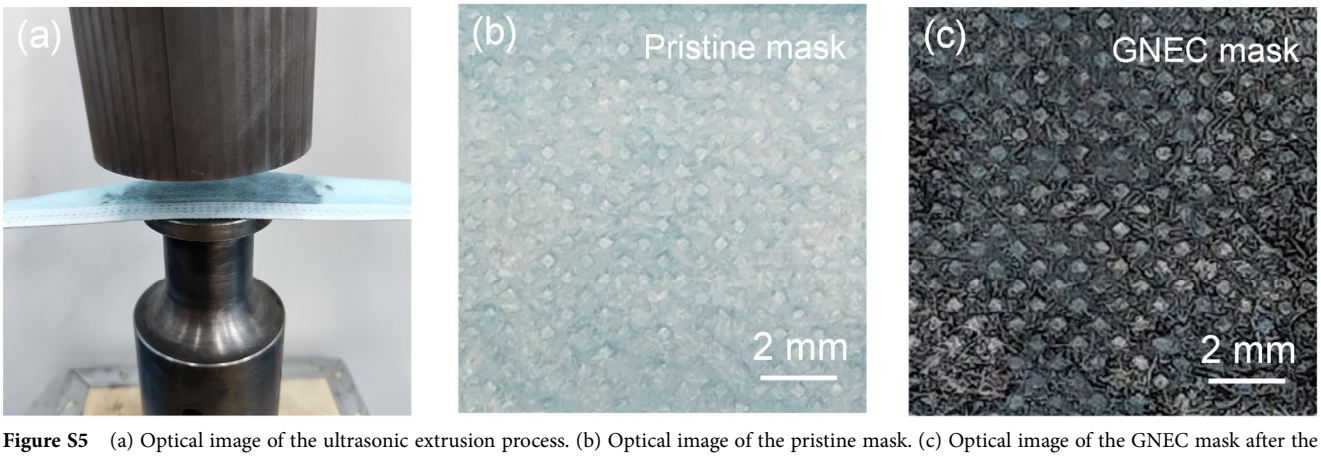

Figure S5 (a) Optical image of the ultrasonic extrusion process. (b) Optical image of the pristine mask. (c) Optical image of the GNEC mask after the ultrasonic extrusion process.

6 The rolling angle of GNEC mask surface

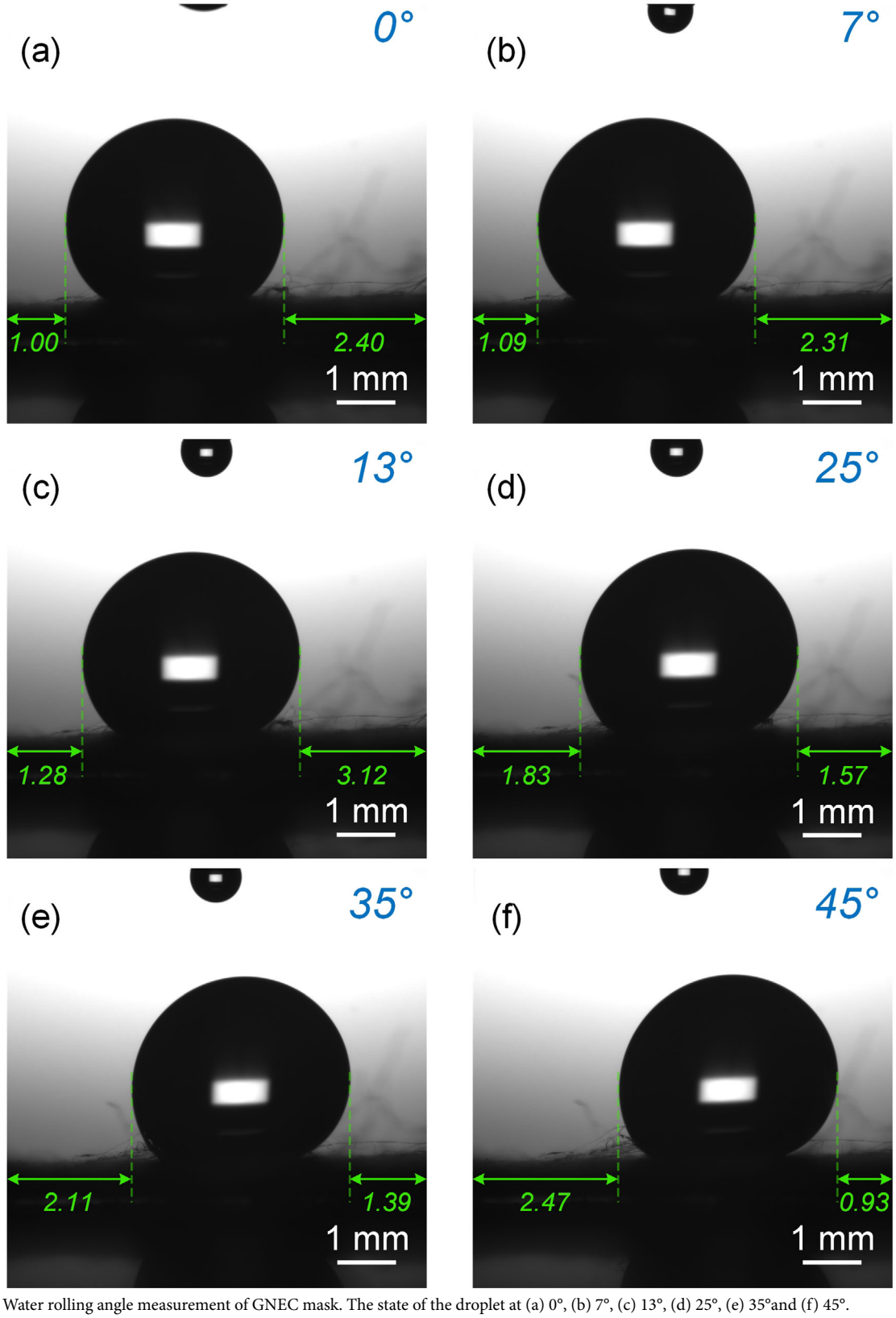

Figure S6 Water rolling angle measurement of GNEC mask. The state of the droplet at (a) 0°, (b) 7°, (c) 13°, (d) 25°, (e) 35°and (f) 45°.

The water contact angle measure platform has a tilt of 90° feature. We measure the water rolling angle by the tilt platform, to simulate the normal use of masks. The tilt angle of the measurement platform is 0° to 90° (tilt speed: 0.5°/s). **Fig. S6** shows the water rolling process of the GNEC mask. At a small inclined angle (7°C) of the platform, the droplets perceptibly roll on the mask surface.

7 The water contact angle of GNEC mask after solar illumination.

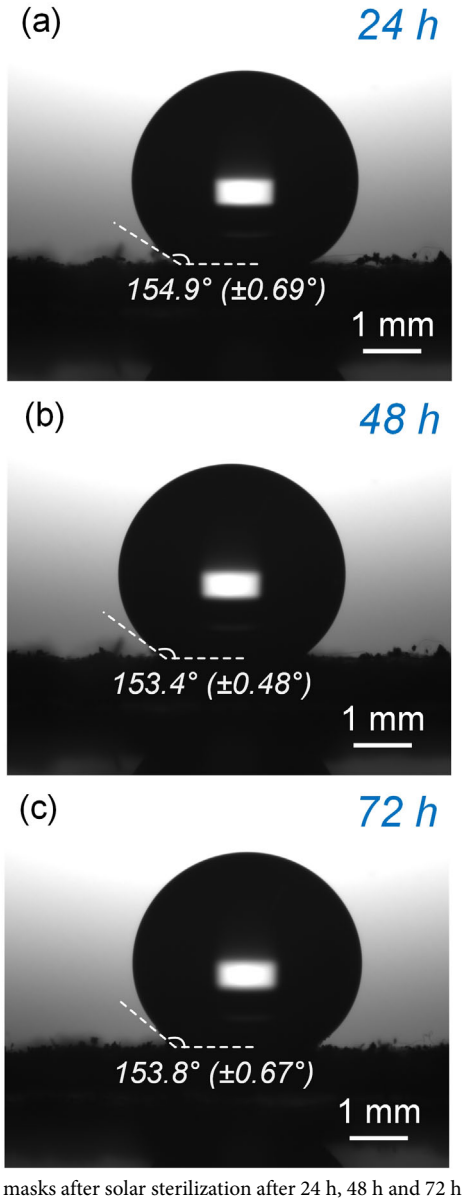

Figure S7 The water contact angle of the GNEC masks after solar sterilization after 24 h, 48 h and 72 h with solar illumination (at 15V input voltage).

Under the long period of solar illumination, the surface hydrophobic feature of the GNEC mask with no declining performances, suggested that the GNEC mask is reusable.

8 Temperature mapping of GNEC mask after 48h illumination.

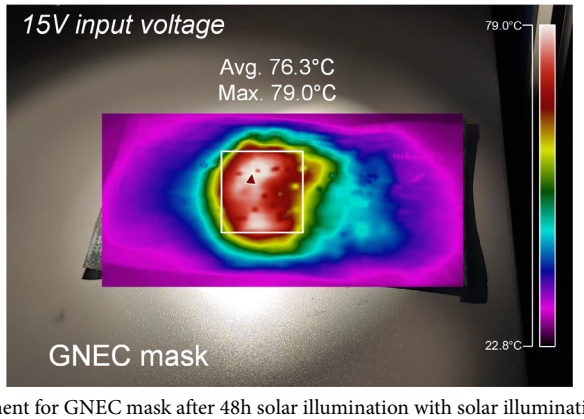

Figure S8 Surface temperature measurement for GNEC mask after 48h solar illumination with solar illumination at (15V input voltage).

9 Air resistance and filter efficiency of GNEC mask after solar illumination.

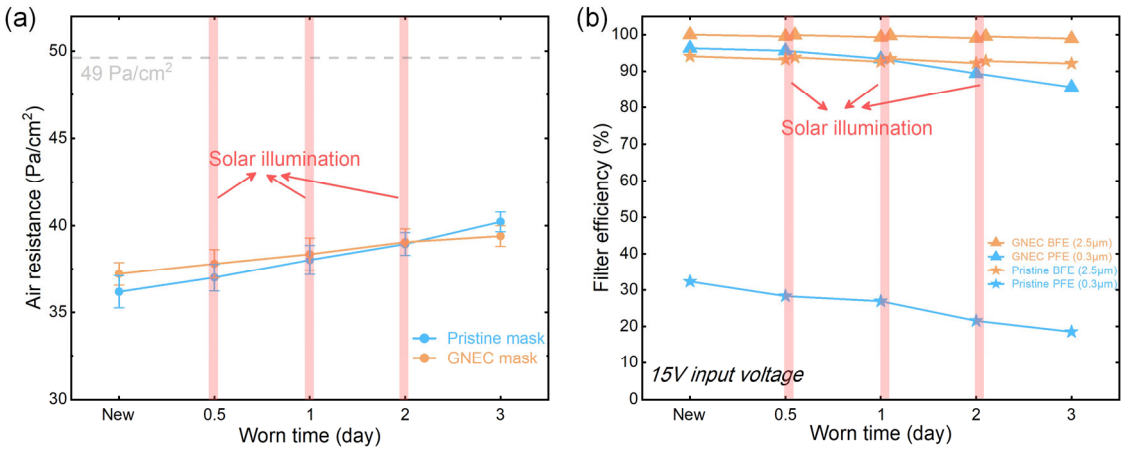

Figure S9 (a) The air resistance of pristine masks and GNEC masks. (b) The cycling experiment of filter efficiency under solar illumination.